

Bayesian inference to characterize Josephson oscillations in a double-well trap

Juha Javanainen and Renuka Rajapakse

Department of Physics, University of Connecticut, Storrs, Connecticut 06269-3046, USA

(Received 26 April 2015; published 11 August 2015)

We use quantum trajectories to simulate Josephson oscillations of atomic condensates between the two sides of a double-well potential. In the simulations the atoms in both wells are monitored using off-resonant light scattering, and the ultimate outcome of our thought experiment is a sequence of photon counts probing the numbers of the atoms in each potential well. We show how to reconstruct the Josephson oscillations from the observed photon counts using Bayesian inference, and study the oscillations quantitatively by averaging the inferred time-dependent oscillation amplitude over a large number of realizations. Scaling behaviors that characterize the oscillations are uncovered and related to physics principles such as measurement back-action. It turns out that the scalings hold true for quite small atom numbers, so that in this sense four atoms in a potential well may already make a Bose-Einstein condensate.

DOI: [10.1103/PhysRevA.92.023613](https://doi.org/10.1103/PhysRevA.92.023613)

PACS number(s): 03.75.Lm, 03.65.Ta, 05.30.Jp

I. INTRODUCTION

Spontaneous symmetry breaking is one of the main organizing principles in condensed-matter physics. Particularly relevant for the present purposes is the notion that a Bose-Einstein condensate (BEC) of atoms is not only characterized by a macroscopic occupation number of a single-particle quantum state, but also has an order parameter akin to a macroscopic wave function associated to it. The order parameter has a global phase that supposedly originates from spontaneous breaking of the “gauge” or U(1) symmetry. The Gross-Pitaevskii equation for a BEC deals with such a macroscopic wave function [1].

A global phase *per se* has no consequences. However, when two condensates with their own phases are allowed to interfere, the interference pattern should depend on the phase difference. This makes at least the phase difference observable. Traditional textbook descriptions [2] of the Josephson effect [3] work this angle: The current carried by tunneling Cooper pairs should depend on the difference of the phases of the order parameter across the tunneling junction.

This idea was transferred early on [4] to a double-well potential that holds two atomic BECs, one on each side, and also permits tunneling between the potential wells. Even if the wells are symmetric and the condensates initially seem identical, as a result of the symmetry-broken phases the atoms should start oscillating back and forth between the potential wells. The amplitude of the oscillations, the fraction of the atoms that get transferred, should depend on the initial phase difference, and should vary at random from experiment to experiment if the condensates are prepared independently with no relation between their phases.

However, theoretical studies of the interference fringes that may or may not ensue when two condensates are overlaid have revealed that no spontaneous symmetry breaking or condensate phase is needed for interference [5–8]. More recent developments of the theme are described in Refs. [9,10]. Formulated in terms of Ref. [5], even if the condensates are initially in number states with nothing to fix the spatial phase for the interference pattern, the correlations unveiled by the measurements of the positions of the individual atoms produce it anyway: While the position of the first detected atom may

be completely random, the correlations built in the state of the system make some positions for the second detected atom more likely than others, and so on. The result is an interference pattern as if the condensates did have phases, albeit phases that vary at random from one run of the interference experiment to the next.

The interference between two condensates was demonstrated experimentally long ago [11], and the interference of an array of condensates has also been studied experimentally [12–14]. The array experiments [12–14] support the picture that the phases of independently prepared condensates are independent random variables that change from one run of the experiment to the next. Curiously, though, there appears to be no explicit experimental demonstration in the literature to the effect that for *two* independently prepared condensates the phases should vary at random.

Since spontaneously broken symmetry is not needed for spatial interference of condensates, the idea is near that the same applies also in the time domain, to the Josephson effect. This was demonstrated theoretically in Ref. [15]. The authors study a double-well potential with atoms inside. In this model the numbers of atoms on both sides of the double well are monitored by scattering of off-resonant light, and the measurement back-action of the monitoring was properly taken into account. Individual experimental runs were modeled using quantum trajectory simulations [16–18]. In each run the expectation values of the atom numbers on the two sides of the double-well potential were shown to oscillate in time in a manner consistent with Josephson oscillations, even if the atoms started in number states on both sides.

The double-well model can be nonlinear in that atom-atom interactions may, for instance, give rise to trapping of the atoms on either side of the trap [19]. Along the lines of Ref. [15] and following leads from a number of earlier analyses of the transition from quantum to classical dynamics [20–23], it may be demonstrated that even such nonlinear dynamics can be derived *ab initio* from linear quantum mechanics using quantum trajectory simulations [24], and that proper modeling of the measurement back-action allows one to discuss the double-well system using nonlinear classical mechanics down to such small atom numbers that, one would think, full quantum mechanics should already be used [25].

There have been clean experimental observations of the dynamics of atoms in two-well systems [26–28]. However, ironically, again we know of no example in which Josephson oscillations in a symmetric trap starting from independent condensates with the same number of atoms on both sides would have been verified experimentally.

Nonetheless, the simulations of the Josephson effect we have mentioned up to now [15,24,25], linear or nonlinear, suffer from a common weakness: The computed quantity is a quantum trajectory, a time-dependent stochastic state vector, and the oscillations of the atoms appear in the *expectation values* of the atom numbers obtained for such a state vector as a function of time. These expectation values have no operational significance, as in the experiments modeled with the quantum trajectories atom numbers are not directly measured. What is observed instead is photon counts coming from two detectors, each of which looks at the light scattered from the atoms in one of the wells.

A large counting rate of light scattered from one well and a simultaneous small counting rate for the other would obviously tell us that the majority of the atoms are in the former well, but this is a rather qualitative observation. In this paper we demonstrate a way to model quantitatively the oscillations of the atoms on the basis of the only data directly available, the photon counts. We employ Bayesian inference [29–31].

We first set up a toy model in which the atoms oscillate sinusoidally back and forth in the double well with some constant amplitude and phase, and the rate of photon counts on each detector is proportional to the square of the number of atoms in each well—square because in our detection model the electric fields of light scattered from the atoms add up, not the intensities. We then devise a Bayesian inference scheme that deduces the amplitude and phase of the oscillations from the photon counts as they keep on accumulating.

Unfortunately, an attempt to apply the same scheme to the photon counts obtained from quantum trajectory simulations of the Josephson oscillations reveals that the inference is what we like to call “stiff”: The apparent amplitude and phase of the Josephson oscillations are not constants, and Bayesian inference that assumes constant values gets increasingly reluctant to follow the changing parameters as more counts accumulate. An inspection of how the inference works reveals the reason, and we may devise a remedy. Basically, the inference continuously narrows the joint probability distribution for the amplitude and phase, while our added algorithm artificially broadens it.

Given a working inference scheme, we may then study the properties of Josephson oscillations. For instance, while the oscillations themselves average out to zero over many experimental realizations, the amplitudes do not, and we may collect statistics about the behavior of, say, the amplitude as a function of time. The main achievement here is that we are able to characterize the Josephson oscillations quantitatively.

The simulations vary in atom number and detection strength, the latter being a measure of the overall rate of photon scattering. The first main observation is that the data fold basically on the same curves when discussed in terms of judiciously chosen dimensionless parameters, such as the number of detected photons per atom. Second, one might think that the Josephson oscillations are a property of the system that emerges in the limit of a large number of atoms, but this turns

out not to be the case: The scalings work all the way down to the level of just a few atoms in the double-well potential. This is yet another example [25,32] where a basically classical model remains valid to unexpectedly low atom numbers.

In the following we expand this narrative with technical details. A discussion of the outcomes concludes the paper.

II. JOSEPHSON OSCILLATIONS

A. Spontaneously broken phase symmetry

We study a symmetric two-well system under the two-mode approximation, or equally well, the two-site version of the Bose-Hubbard model. The Hamiltonian is

$$\frac{H}{\hbar} = -J(a^\dagger b + b^\dagger a) + U(a^\dagger a^\dagger a a + b^\dagger b^\dagger b b), \quad (1)$$

where a and b are the boson operators for the atoms at the two sites, J characterizes the tunneling between the wells, and U is a measure of the on-site atom-atom interactions. From now on, though, we only consider noninteracting atoms and set $U = 0$. Generically speaking, we assume that there is a large number of atoms on both sides of the trap, and think of the bosons as making a condensate in each side of the trap.

In the usual way one may find a semiclassical version of the two-well problem by taking the Heisenberg equations of motion of the boson operators and declaring that, instead of the boson operators a and b , we have c -number quantities α and β . We then have

$$\dot{a} = iJb, \dot{b} = iJa; \quad \dot{\alpha} = iJ\beta, \dot{\beta} = iJ\alpha. \quad (2)$$

From here on we denote the total atom number by N . For simplicity of the discussion we always take it to be an even integer. The atom number operator $N = a^\dagger a + b^\dagger b$ is conserved in quantum theory, and so is its counterpart in the semiclassical approach, $N = \alpha^* \alpha + \beta^* \beta$.

Suppose the semiclassical description starts at $t = 0$ with exactly half of the atoms in each trap, and that the condensates have the phases $\phi_{a,b}$. This means that initially we have

$$\alpha = \sqrt{\frac{N}{2}} e^{i\phi_a}, \quad \beta = \sqrt{\frac{N}{2}} e^{i\phi_b}. \quad (3)$$

It is easy to work out the expression for what we here and below call population imbalance,

$$z(t) = \frac{|\beta|^2 - |\alpha|^2}{N} = \sin \Phi \sin 2Jt. \quad (4)$$

The atoms thus oscillate back and forth between the traps at the angular frequency $2J$, and the amplitude of the oscillations depends on the initial phase difference $\Phi = \phi_b - \phi_a$.

One way of formulating the quantum problem is in terms of the expectation values of the atom numbers. Assume that in the initial state at $t = 0$ the expectation values of atom numbers and the cross-expectation value read

$$\langle a^\dagger a \rangle = \langle b^\dagger b \rangle = \frac{N}{2}, \quad \langle a^\dagger b \rangle = \frac{N}{2} e^{i\Phi}. \quad (5)$$

This would be the case if the system started with the bosons in the a and b modes in coherent states with the corresponding coherent-state parameters $\sqrt{\frac{N}{2}} e^{i\phi_a}$ and $\sqrt{\frac{N}{2}} e^{i\phi_b}$ with $\Phi = \phi_b - \phi_a$. Now, the atom number in a coherent state

is indeterminate, but the same expectation value of $\langle a^\dagger b \rangle$ also results more plausibly from a so-called phase state in which the total atom number in the double-well trap is fixed [9,10]. Either way, the population imbalance expressed in terms of quantum-mechanical expectation values becomes

$$z(t) = \frac{\langle b^\dagger b \rangle - \langle a^\dagger a \rangle}{N} = \sin \Phi \sin 2Jt. \quad (6)$$

The standard assumption in boson systems in fact is that the “gauge” or phase symmetry is spontaneously broken in a BEC, so each of the condensates on the two sides of the double well should have some definite phase. We then expect something like $\langle a^\dagger b \rangle = \frac{N}{2} e^{i\Phi}$ to hold true, and oscillations should result. This was the essence of the original argument for the oscillations of the condensates between the two sides of the trap as in Ref. [4]. However, one would rather think that independent initial preparation of the condensates would produce gases with definite (even if unknown) atom numbers, i.e., number states. Then the cross-expectation value must be $\langle b^\dagger a \rangle = 0$, and no oscillations should ensue. The issue of Josephson oscillations forcefully arises when we assume that the two bosonic modes start out in the number states with $N/2$ atoms on each side, and ask if there will be oscillations.

We have reason to believe that Josephson oscillations would take place in spite of the seeming inconsistency in the quantum-mechanical prediction. The crux is that a quantum-mechanical expectation value stands for the average over a large number of experiments. If the atom numbers in the traps could be followed as a function of time in an individual run of an experiment, there is nothing to preclude Josephson oscillations. The agreement with the quantum-mechanical expectation values can be restored because the seeming initial phase difference Φ varies at random from one run of the experiment to the next, and over many experiments the oscillations would average out. This is the angle we pursue here.

B. Measurements produce oscillations

As was shown in Ref. [15], there should be Josephson oscillations. The argument has two legs. First, suppose far-off resonant light is shone on the condensates, and the light scattered from each well is collected separately. Assuming mode matching between the condensates and the detection light, the fields from each atom add. A measuring device whose response is proportional to the intensity of light therefore sees a signal that is proportional to the square of the number of atoms. The back-action of the detection in such a measurement is reasonably modeled by a Lindblad form [33,34] Liouville superoperator \mathcal{L} that maps the density operator of the two-well system as

$$\mathcal{L}\rho = \sum_{i=a,b} [L_i \rho L_i^\dagger - \frac{1}{2}(\rho L_i^\dagger L_i + L_i^\dagger L_i \rho)], \quad (7)$$

with $L_a = \sqrt{\Gamma} a^\dagger a$ and $L_b = \sqrt{\Gamma} b^\dagger b$. Here Γ is a parameter that governs the strength of the measurement, and of the back-action as well. It may be adjusted by adjusting the tuning and the intensity of the detection light. The full equation of motion of the density operator of the atoms in the two potential wells

reads

$$\dot{\rho} = -i[H/\hbar, \rho] + \mathcal{L}\rho. \quad (8)$$

The management of the numerical solution of Eq. (8) and sorting-out of the results is achieved most easily if the analysis employs properly chosen dimensionless quantities. One natural unit is the period of the expected Josephson oscillations. The (angular) frequency of the oscillations should be $2J$, so the oscillation period is π/J . In our final results we therefore express the running time t in terms of the dimensionless quantity

$$\tau = \frac{Jt}{\pi} \quad (9)$$

that counts the periods of the expected Josephson oscillations. On the other hand, a representative number of atoms on both sides of the trap is $N/2$ and a characteristic rate of the emission of photons from each trap is $\Gamma(N/2)^2$. Instead of the rate Γ we therefore use the typical number of photons emitted from each well during a period of the Josephson oscillations,

$$\gamma = \frac{\pi \Gamma N^2}{4J}, \quad (10)$$

to quantify the strength of the detection. The variables τ and γ will indeed neatly remove much of the dependence on the parameters N and J from the problem. We continue to display N , Γ , and t in our development, but the results are usually expressed in terms of γ and τ .

As was also done in Ref. [15], as the second leg of the argument we solve the master equation (8) by means of quantum trajectory simulations [16–18]. The idea is to find a swarm of stochastically evolving state vectors $|\psi(t)\rangle$, quantum trajectories, so that when one calculates the expectation value of any system observable at any particular time for each quantum trajectory and averages the result over the quantum trajectories in the swarm, the result approximates the result that would be obtained by directly solving the master equation (8) of the density operator and calculating the expectation value from the density operator.

Here we employ a numerically efficient version [17,34] of the simulations that runs as follows. We start every trajectory from a number state with half of the atoms in each potential well. Two types of time evolution will occur. First, the state vector evolves under the non-Hermitian effective Hamiltonian

$$H_E = H - \frac{1}{2}\hbar\Gamma[(a^\dagger a)^2 + (b^\dagger b)^2]. \quad (11)$$

This evolution shrinks the norm of the state vector, which leads to the second type of evolution. Namely, given a normalized initial state, we first pick a uniformly distributed random number $\xi \in (0,1)$. We then integrate the time-dependent Schrödinger equation for the state vector $|\psi(t)\rangle$ under the effective Hamiltonian (11) up to a time such that the norm has reached the value ξ . At this time a “quantum jump” takes place. With the respective probabilities

$$P_a = \frac{\langle \psi | (a^\dagger a)^2 | \psi \rangle}{\langle \psi | (a^\dagger a)^2 | \psi \rangle + \langle \psi | (b^\dagger b)^2 | \psi \rangle}, \quad P_b = \dots \quad (12)$$

the algorithm picks the state to be $|\psi\rangle_a = a^\dagger a |\psi\rangle$ or $|\psi\rangle_b = b^\dagger b |\psi\rangle$. The state is then normalized, a new random number ξ is picked, and the algorithm starts over. In practice we have

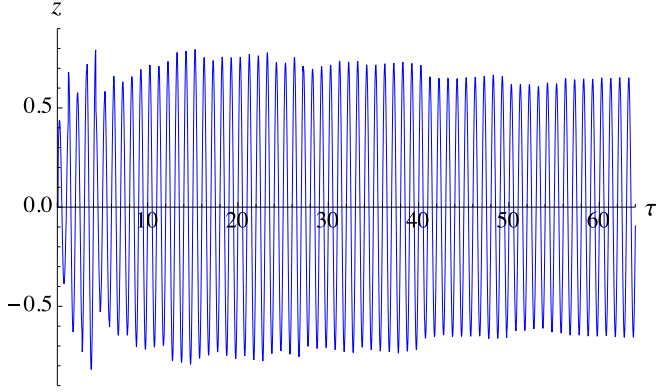


FIG. 1. (Color online) Population imbalance z as a function of dimensionless time τ for a single quantum trajectory. The parameters are particle number $N = 128$ and dimensionless detection strength $\gamma = 10$.

performed some surgery on Numerical Recipes [35] adaptive-stepsize differential equation solvers so that the driver routine finds the solution to the equation $\langle \psi(t) | \psi(t) \rangle = \xi$ internally, and simply restarts the integration at that time.

At this point we have a swarm of quantum trajectories. Now, since we have a time-dependent (albeit unnormalized) state vector $|\psi(t)\rangle$ for each trajectory, there is nothing to prevent us from formally computing the population imbalance $z(t)$ as in Eq. (6) for it. The operational significance of this $z(t)$ is hazy since a comparison with prediction and experiment would then call for repeated experiments with the same quantum trajectory $|\psi(t)\rangle$ prepared over and over again. However, the trajectory is just a formal construct to solve the master equation, and the proper averaging should involve averaging over the members of the swarm of quantum trajectories derived from different random numbers ξ in each simulation, not averaging over the same single trajectory.

Nevertheless, the simplified average produces Josephson oscillations in $z(t)$ that (for suitable measurements strengths) are at least in qualitative accord with the symmetry breaking arguments [15]. For an example, see Fig. 1 that presents the population imbalance as a function of the dimensionless time τ for the detection strength $\gamma = 10$. Here the atom number is $N = 128$. After an initial startup, the imbalance evidently suggests back-and-forth oscillations of the atoms between the two potential wells.

The final argument that puts the quantum trajectory simulations on a firm basis follows from the (highly idealized) assumption that every scattered photon is also detected on a photodetector. We take it from the discussions in, say, Refs. [31,34] that the statistics of the quantum jumps in one run of the simulation is exactly the same as the statistics of photon detection events in one run of the corresponding experiment. A quantum trajectory simulation should therefore be a faithful simulation of an experiment: each quantum jump corresponds to detection of a photon. Besides, in the scheme we have thus described, the detected photons are the actual and exclusive outcome of a single experiment, not the somewhat fictitious imbalance $z(t)$. The question that we must pose is then about the relation between the oscillations of the atoms and the

photon counts on the detectors: How to infer continuous oscillations of the atoms from the discrete photon counts?

III. BAYESIAN INFERENCE OF OSCILLATIONS

A. Analyzing steady oscillations

To get a handle on the photon counts, we begin with a simple model saying that the atoms oscillate sinusoidally back and forth between the traps so that the population imbalance behaves as

$$z(t) = A \sin(2Jt + \phi), \quad (13)$$

where A and ϕ are the constant amplitude and phase of the oscillations. Moreover, we assume a detection strength such that the instantaneous rate of photon counts on each detector is Γ times the square of the number of atoms in each potential well. The probability of a photon count on each detector over a short time interval Δt is therefore

$$P_{a,b} = \frac{\Delta t N^2 \Gamma}{4} [1 \mp z(t)]^2. \quad (14)$$

The meaning of the parameter Γ here is precisely the same as in the quantum trajectory simulations. We take the time step Δt to be so small that the probability for more than one detected photon during Δt is very small, and divide time into intervals of width Δt that we label by, say, their final times: $t_n = n \Delta t$, $n = 1, 2, \dots$; $t_0 = 0$ is reserved for the initial time.

1. Bayesian inference

Suppose we generate a random sequence of detection events according to the probabilities (14) at times t_n . For an asymptotically small time step Δt the most likely outcome actually is that there is no photon detection, which occurs with the probability

$$P_0 = 1 - P_a - P_b, \quad (15)$$

but occasionally we do have either an a or a b count. Let us collectively denote these three outcomes as c , and the outcome at time t_n as c_n .

Knowing the parameters N , Γ , and J it is possible to backtrack the parameters of the oscillations A and ϕ from the synthesized photon counts or the absence thereof, c_n , using Bayesian inference; see, e.g., [29,30]. The basic idea is simple and well known. Regard the parameters $A \in [0, 1]$ and $\phi \in [0, 2\pi)$, collectively $p \in [0, 1] \times [0, 2\pi)$, also as random variables. Equations (14) and (15) may then be viewed as specifying the conditional probability for the experimental outcome c given the parameter value p , $P_n(c|p)$. Here the probability law depends on the time step through the time dependence in Eq. (14). The famous Bayesian formula expresses the probability for the parameter value p conditioned on the experimental outcome c , $P_n(p|c)$ as

$$P_n(p|c) = \frac{P_n(c|p)P_n(p)}{P_n(c)}, \quad (16)$$

where $P_n(p)$ and $P_n(c)$ are the unconditional probabilities for the parameters and experimental outcomes at the time step n .

Assume now that at time t_n we have an estimate for the probabilities of the parameters p , $P_n(p)$. If an experiment during the next time step produces the outcome c_{n+1} , the

updated probability distribution for the parameters at time t_{n+1} is the one conditioned on this outcome c_{n+1} . We therefore have

$$P_{n+1}(p) = P_{n+1}(p|c_{n+1}) = \frac{P_{n+1}(c_{n+1}|p)P_n(p)}{P_{n+1}(c_{n+1})} \\ = K_{n+1}P_{n+1}(c_{n+1}|p)P_n(p), \quad (17)$$

where K_{n+1} is independent of p and may simply be chosen after the fact so that the $P_{n+1}(p)$ for all p add up to 1. We assume that initially we have no knowledge of the values of the parameters A and ϕ and set an even distribution for them over the intervals $A \in [0, 1]$ and $\phi \in [0, 2\pi)$ as the initial distribution $P_0(p)$.

2. Numerical details

In practical implementations the generation of photon counts and the inference are separate issues, and one may well use different time steps for each. From now on we assume that the generation and the analysis of the photon counts are decoupled in this manner. As far as the inference is concerned the only question is whether there is a count in the detection interval Δt , and if so, is it an a or a b count. Now, since we know that the characteristic rate of the counts in each channel is $N^2\Gamma/4$, the expected number of counts in each time step and in each channel is approximately $N^2\Gamma\Delta t/4$. This means that for each channel we go on the average about

$$s = \frac{4}{N^2\Gamma\Delta t} = \frac{\pi}{\gamma J\Delta t} \quad (18)$$

time steps between the jumps. This is another convenient dimensionless variable that seems to correctly capture a scaling in the problem.

In our examples we always use $s \geq 20$; the code determines the actual value from other considerations such as the time step we wish to use to plot the results. In this way the time step for inference appears to work well in practice. Nevertheless, whatever value of the time step, it may happen that there is more than one count during any particular time step of the inference anyway. In such a case our code keeps on halving the inference time step recursively until only at most one count is found in each reduced time step. For instance, suppose that there are initially two counts in an interval and after the halving both counts are still in one of the half-intervals. Then the half-interval without counts is kept as is and the half-interval with two counts is halved again. Naturally, one cannot store continuous-valued probability distributions, which must be discretized for numerical purposes. Below we always use $n_A = 101$ equidistant values of A , as in $0, 0.01, \dots, 1.00$, and $n_\phi = 100$ values of ϕ , as in $0, 0.01 \times 2\pi, \dots, 0.99 \times 2\pi$. The statistical fluctuations of A and ϕ in the runs of Bayesian inference giving the final results of this paper are at least a few times larger than the discretization steps.

The joint probability distribution of A and ϕ tends to get more tightly confining with an increasing number of time steps, and numerical underflow has proven to be a distinct possibility outside of the high-probability region of A and ϕ . That is why we actually store the logarithm of the probability distribution of the parameters A and ϕ , not the distribution itself.

The final issue is how one should read out the results of the inference. Three alternatives were used in this work for the

oscillation amplitude. First, we may simply calculate the mean value of the amplitude A_E (E as in ‘‘expectation value’’) from the joint probability distribution $P_n(p)$ of A and ϕ . Second, we may compute the marginal distribution of the variable A and report the most probably value A_M for it. Third, we may use the average of the two, $A_A = \frac{1}{2}(A_E + A_M)$. Obviously, the narrower the probability distribution gets, the smaller is the difference between these alternatives. In the analysis of simulations of actual Josephson oscillations as described in Sec. III B 1 below we have noticed that the expectation value A_E tends to avoid the extreme amplitudes 0 and 1 and the most probable value A_M tends to get stuck at them. From now on we therefore always report inference results in terms of the average of the two, A_A , which partly cures both ills, and denote it simply by A . The standard deviation in the inference σ_A is, when needed, obtained from the probability distribution $P_n(p)$.

For the phase ϕ we use a process that takes into account the fact that phases separated by an integer multiple of 2π are equivalent to estimate the mean and standard deviation of the phase from the probability distribution $P_n(p)$,

$$\phi_E = \arg \langle e^{i\phi} \rangle, \quad \sigma_\phi = \sqrt{-\ln |\langle e^{i\phi} \rangle|^2}. \quad (19)$$

There are no extreme values for the phase, no associated problems, and no remedies. We report ϕ_E , and denote it by ϕ .

3. Example on Bayesian inference

The process of inference is illustrated in Fig. 2. We set $A = 0.7$ and $\phi = 0$, and generate a sequence of counts according to Eqs. (14) and (15) for the detection strength $\gamma = 5$ using a very small time step. The upper graph shows the original

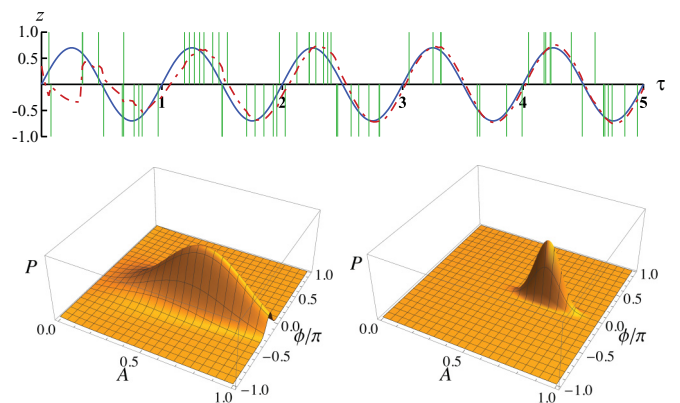


FIG. 2. (Color online) Upper: Sinusoidal oscillations over five periods (solid blue line), counting events synthesized according to Eq. (14) represented with bars from 0 to 1 for detector b and from 0 to -1 for detector a (solid green lines), and the predicted oscillations using the values of the parameters of the oscillations A and ϕ inferred as the counting events accumulate (dot-dashed red line). The actual values of the parameters were $A = 0.7$ and $\phi = 0$, and the detection strength was $\gamma = 5$. Lower: The probability distribution P of the parameters A and ϕ from Bayesian inference at times $\tau = 1$ (left) and $\tau = 10$ (right). The distributions are unnormalized and scaled to the same maximum value. There are a few unusually thick green vertical bars because of two counts that are not resolved in the figure.

oscillations (solid blue line) and the counting events for the two detectors (vertical green bars). Also shown are the “predicted” oscillations obtained from Eq. (13) using the values of A and ϕ that are continuously updated as the inference proceeds (dot-dashed red line). At the bottom we have the unnormalized probability distributions for the parameters A and ϕ from Bayesian inference after $\tau = 1$ and $\tau = 10$ periods of the sinusoidal oscillations. Evidently the inference has found a reasonably good estimate for the parameters already after one period of the oscillations, after a total of about ten recorded counts, and the inference gets increasingly accurate as the counts keep on accumulating.

B. Analyzing simulated photon counts

The previous Sec. III A showed how the Bayesian inference works with an artificial test signal corresponding to steady oscillation of the atoms between the traps. We next apply the inference to analyze the photon counts (quantum jumps) from quantum trajectory simulations. The hypothesis is that the atoms actually oscillate back and forth and the photon counts obey the description of Eqs. (13)–(15). The goal is to find the amplitude and phase of the oscillations from the photon count data.

The problem one may immediately anticipate in view of Fig. 1 is that the simulated photon counts do not correspond to oscillations of the atoms with a constant amplitude, and possibly not a constant phase either. In fact, we have found that, as time goes on, the straightforward Bayesian inference becomes stiff; the inferred amplitude follows the changes of the oscillations in the computed population imbalance $z(t)$ with a pronounced lag; see Fig. 3 below. The reason is easy to see. Suppose for the sake of the argument that the phase remains a known constant and we only need to consider changes in the amplitude A . Then, along a stretch when the amplitude stays approximately constant, the amplitude distribution $P_n(A)$ gets increasingly sharply peaked. When the amplitude changes, the Bayesian algorithm multiplies such a sharply peaked distribution of A with probabilities $P_{n+1}(c_{n+1}|A)$ that vary slowly as a function of the variable A , and it takes many Bayesian steps to move the probability distribution of A around to accommodate the new value of the amplitude.

1. Amending Bayesian inference

We have come up with a physically motivated *ad hoc* remedy for the stiffness: Since the narrowing of the probability distribution causes the problem, let us add some diffusion to the dynamics of the probability distribution to broaden it artificially. The multiplications by $P_{n+1}(c_{n+1}|p)$ may then have a larger effect on the probability distribution of the parameters than they would have without the broadening.

The specifics for the amplitude distribution run as follows. Let the n_A points at which the amplitude distribution is stored at the intervals $\Delta A = 1/(n_A - 1)$ be $A_n = n \Delta A$, $n = 0, \dots, n_A - 1$, and the corresponding values of the probabilities of A_n for each fixed phase ϕ be p_n . The broadening after each time step is governed by a parameter $0 < g_A < \frac{1}{2}$ in such

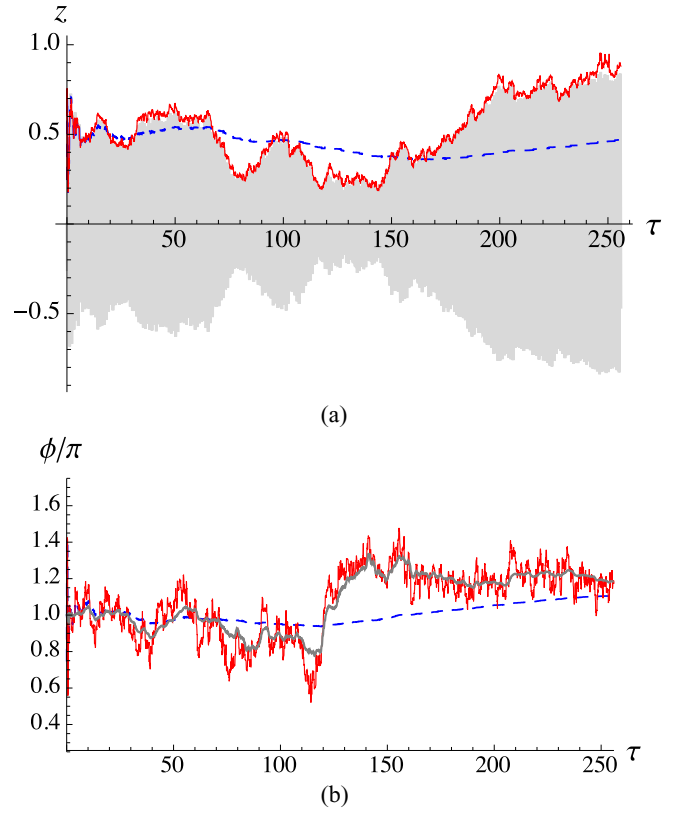


FIG. 3. (Color online) (a) Oscillations of the computed population imbalance z as a function of time τ in a particular quantum trajectory (gray area), the amplitude A inferred without the broadening algorithm (dashed blue line), and with the broadening algorithm described in the text (solid red line). (b) Similarly for the inferred phase. The solid grey line $\phi(\tau)$ in the phase panel (b) is obtained from a sliding fit of the oscillations of $z(\tau)$ to the form $A \sin(2\pi \tau + \phi)$ over the range of τ of width 2π centered at the argument τ . The parameters are $N = 128$, $\gamma = 4$.

a way that we have

$$\begin{aligned}
 p_0 &\rightarrow \bar{p}_0 = \left(1 - \frac{1}{2}g_A\right)p_0 + \frac{1}{2}g_A p_1; \\
 p_n &\rightarrow \bar{p}_n = \frac{1}{2}g_A p_{n-1} + \left(1 - g_A\right)p_n + \frac{1}{2}g_A p_{n+1}, \\
 &\quad n = 1, \dots, n_A - 2; \\
 p_{n_A-1} &\rightarrow \bar{p}_{n_A-1} = \frac{1}{2}g_A p_{n_A-2} + \left(1 - \frac{1}{2}g_A\right)p_{n_A-1}. \quad (20)
 \end{aligned}$$

After the broadening step is done, we use the new values \bar{p}_n as the probability distribution $\{p_n\}$.

This broadening preserves the total probability $\sum_n p_n$. Moreover, suppose we start with a probability distribution such that $p_n = \delta_{n,n_0}$ for some n_0 close to the center of the grid of the A values. After one broadening step we have the values $p_{n_0-1} = p_{n_0+1} = \frac{1}{2}g_A$, $p_{n_0} = 1 - g_A$. The expectation value of the index n after one step therefore is $\langle n \rangle = n_0$, and the variance is $(\Delta n)^2 = g_A$. Next imagine repeating the broadening step for some total number of times n_g without any other intervening operations. As long as the spreading distribution $\{p_n\}$ does not extend to the ends of the grid at $n = 0$ and $n = n_A - 1$, the average remains $\langle n \rangle = n_0$, the variances add up to $(\Delta n)^2 = n_g g_A$ and, as one would expect from the central limit theorem, the distribution $\{p_n\}$ in fact approaches

a Gaussian distribution in n . The broadening indeed acts like diffusion, adding $n_g g_A$ to the variance of the A distribution in n_g steps.

Let us continue for the time being with the hypothetical example about the broadening being the sole reason for the evolution of the probability distribution. One sees that if the broadening distribution collides with the edges of the grid for the amplitudes A , the expectation value of A is no longer preserved and is expected to be biased away from the extremely values 0 and 1. Likewise, the collision of the spreading probability distribution with the edges should artificially increase the probability of the extreme values. These are the obvious explanations for our observations that with added broadening of the probability distribution the mean value of A seems to be biased away from 0 and 1 and the most probable value of A is unduly biased toward 0 or 1. As we already noted in Sec. IIIA2, this is our motivation for reporting the average of the mean and most probable value of the amplitude as the result of the inference.

We carry out an analogous broadening of the phase distribution for each Bayesian step after having performed the broadening of the amplitude distribution. The broadening algorithm for the phase with the indices $n = 0, \dots, n_\phi - 1$ reads

$$p_n \rightarrow \bar{p}_n = \frac{1}{2} g_\phi p_{n-1} + (1 - g_\phi) p_n + \frac{1}{2} g_\phi p_{n+1}. \quad (21)$$

Since the phase wraps around, here we simply interpret $p_{n_\phi} = p_0$, $p_{-1} = p_{n_\phi - 1}$.

2. Numerical details

To obtain a parameter-invariant measure of the spreading, suppose that we take an average of s steps between successive counts in one of the channels. Then the typical added standard deviation of the A distribution between successive counts is

$$\Sigma_A = \Delta A \Delta n = \frac{1}{n_a - 1} \sqrt{s g_A}. \quad (22)$$

This means that, for a desired value Σ_A , we want to put in the broadening parameter

$$g_a = \frac{(n_a - 1)^2 \Sigma_A^2}{s}. \quad (23)$$

A similar reasoning applies to the phase. To have the standard deviation from s steps to be the fraction Σ_ϕ of the total range 2π of the phase, we have in exact analogy with Eq. (23)

$$g_\phi = \frac{n_\phi^2 \Sigma_\phi^2}{s}. \quad (24)$$

For our standard choice of parameters we have $n_\phi = n_A - 1 = 100$. After some experimenting we have found that $\Sigma_A = 0.02$, $\Sigma_\phi = \sqrt{2} \Sigma_A$ constitute a reasonable compromise between unnecessary spreading of the amplitude and phase distributions and stiffness in the inferred parameters. In order not to hamper initial convergence we have also installed limiter values of the relative standard deviations S_A and S_ϕ such that the broadening sets in softly only after the standard deviations of amplitude and phase, σ_A and σ_ϕ , fall below these values:

$$\begin{aligned} g_A &\rightarrow 0, & \sigma_A &\geq S_A, \\ g_A &\rightarrow \left(1 - \frac{\sigma_A}{S_A}\right) g_A, & \sigma_A &< S_A, \end{aligned} \quad (25)$$

and similarly for the phase. The parameters S_A and S_ϕ appear not to be very critical, and presently we simply set

$$S_A = S_\phi = \frac{2}{\sqrt{n_\phi}}. \quad (26)$$

In very round numbers, the resulting relative standard deviations (standard deviation/range of parameter) of both amplitude and phase in the probability distribution $P_n(p)$ during the Bayesian inference tend to be in the few percent range.

3. Example on modified inference

We illustrate the concepts discussed in the present Sec. III B in Fig. 3. In Fig. 3(a) we first plot the oscillations in the computed population imbalance z for one particular quantum trajectory. Here we picked a simulation run that is unusually challenging for Bayesian inference. The time runs up to $\tau = 256$ and the plot covers 256 expected Josephson oscillations, so the oscillations of $z(\tau)$ are not resolved and appear as gray blur. The dashed blue line is the amplitude A from unmodified Bayesian inference, and demonstrates the stiffness of this method. The solid red line is the amplitude A obtained from Bayesian inference with added broadening of the parameter distribution as described in this section, Sec. III B, and in this example it tracks the tops of the oscillations of $z(\tau)$ quite well. Finally, Fig. 3(b) shows the phase ϕ as a function of time τ for this particular quantum trajectory, both from raw inference (dashed blue line) and with the added broadening of the inference algorithm (solid red line). The phase ϕ deduced from the oscillations of $z(\tau)$ is also shown as the solid gray line. It fluctuates notably less than the phase found from Bayesian inference with the added broadening algorithm.

IV. RESULTS

We now have the tools to characterize the Josephson oscillations. As illustrated by Figs. 1 and 3, the result for each run of an experiment or quantum trajectory simulation is not only random, literally, but may vary enormously in character. We need to average over trajectories to gain an overall picture of the Josephson oscillations. Averaging the imbalances $z(t)$ over a large number of runs would produce effectively zero, not to mention that $z(t)$ is not directly observable anyway. However, we may infer the oscillation amplitude A for each run as a function of time, and profitably average these over a large number of runs. In our examples below, with averaging, the average $\langle A \rangle$ is always over 1024 trajectories. This still leaves easily discernible statistical fluctuations in the averages.

One example is shown in Fig. 4. Here we plot the averaged $\langle A \rangle$ for two different atom numbers, $N = 256$ (solid red line) and $N = 64$ (dashed blue line). The horizontal axis is the scaled time τ , and the observation strength is $\gamma = 1$.

Two features are found. First, with increasing running time τ the average $\langle A \rangle$ rises quickly to approximately the same common value regardless of the atom number. Although this is not visible on the time scale plotted in Fig. 4, here the initial rising part of $\langle A \rangle(\tau)$ is materially the same for both atom numbers. Second, with increasing time, the averages continue

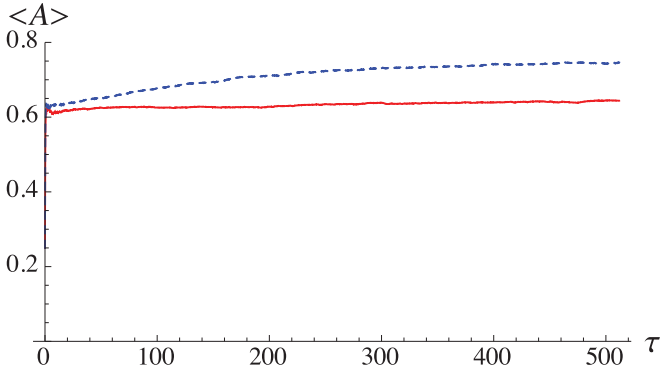


FIG. 4. (Color online) Oscillation amplitude averaged over 1024 quantum trajectories $\langle A \rangle$ as a function of the number of nominal periods of Josephson oscillations τ . Two different atom numbers are used, $N = 256$ (solid red line) and $N = 64$ (dashed blue line). Here the parameter characterizing the detection strength, comparable to the expected number of detection events per one period of Josephson oscillations, equals $\gamma = 1$.

to rise slowly, the more slowly the larger is the number of the atoms.

Let us now return to the most naive picture of the Josephson oscillations, as in Eqs. (4) or (6). The amplitude of the oscillations depends on the initial phase difference Φ as $|\sin \Phi|$. If the phase difference Φ is a uniformly distributed random variable, the average amplitude is

$$\langle |\sin \Phi| \rangle = \frac{1}{\pi} \int_0^\pi d\Phi \sin \Phi = \frac{2}{\pi} \simeq 0.637. \quad (27)$$

This is conspicuously close to the value where the average amplitude $\langle A \rangle$ plateaus after the initial rise. We have not drawn the value $2/\pi$ in Fig. 4 as a horizontal line simply because it would all but obscure the solid red line for $N = 256$. The elementary classical picture of Josephson oscillations gives a nontrivial quantitative prediction, which is confirmed in our simulations.

Next consider the initial rise of $\langle A \rangle(\tau)$ in detail. In Fig. 5 we plot the short-time rise of the average amplitude for the atom number $N = 128$ for two different detection strengths

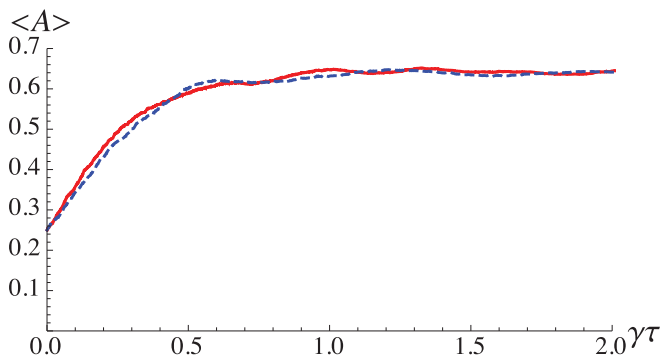


FIG. 5. (Color online) Short-time rise of the average amplitude $\langle A \rangle$ for the atom number $N = 128$ for two different detection strengths $\gamma = 1/\sqrt{2}$ (solid red line) and $\gamma = \sqrt{2}$ (dashed blue line) as a function of the expected number of detection events in each channel $\gamma\tau$.

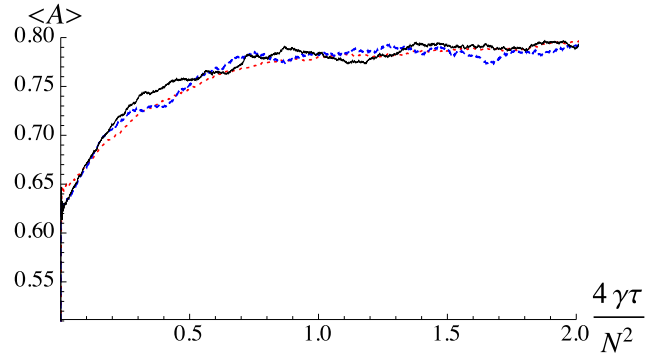


FIG. 6. (Color online) $\langle A \rangle$ as a function Γt for $N = 32$, $\gamma = 2$ (dotted red line), $N = 64$, $\gamma = 2$ (dashed blue line), and $N = 64$, $\gamma = 8$ (solid black line). The horizontal axis is labeled with the same dimensionless quantities as were used in other figures; $4\gamma\tau/N^2 = \Gamma t$.

$\gamma = 1/\sqrt{2}$ (solid red line) and $\sqrt{2}$ (dashed blue line) not as a function of the scaled time τ , but as a function of the expected number of detection events in each channel $\gamma\tau$. The two curves are virtually on top of one another, and the final value of $\langle A \rangle \simeq 2/\pi$ is reached for $\gamma\tau \sim 1$. There is a dead time in the beginning before the inference kicks in, but on the average it only takes on the order of one photon detection in each channel before the Bayesian inference will start reporting meaningful values for the amplitude of the Josephson oscillations.

Incidentally, one may wonder why at $\tau = 0$ we have $\langle A \rangle(\tau) = 1/4$. The reason is that for the initial uniform distribution over $[0, 1]$, the average of A is $A_E = 1/2$, and the way our algorithm for the most probable value of A works, it declares the value $A_M = 0$; hence $A = \frac{1}{2}(A_E + A_M) = 1/4$. The number $1/4$ is not particularly significant, but the time it takes $\langle A \rangle(\tau)$ to evolve away from $1/4$ to a new approximately stationary value is.

This leaves the continuing slow rise of $\langle A \rangle(\tau)$ seen in the dashed blue line for $N = 64$ in Fig. 4. To this end we plot $\langle A \rangle$ not as a function of the number of periods in Josephson oscillations τ , but as a function of another dimensionless variable Γt ; in terms of our dimensionless variables, $\Gamma t = 4\gamma\tau/N^2$. We present three graphs of this kind in Fig. 6 for the parameters $N = 32$, $\gamma = 2$ (dotted red line), $N = 64$, $\gamma = 2$ (dashed blue line), and $N = 64$, $\gamma = 8$ (solid black line). Evidently we have once more caught a correct scaling in the problem.

The qualitative picture we develop is that Josephson oscillations set in as expected from the naive semiclassical symmetry breaking argument in Sec. II A. However, we do not see them directly but only through discrete photon counts, and so it takes about one photon count in each channel to begin detecting the oscillations. Moreover, we hypothesize that the further gradual increase in the amplitude is due to measurement back-action. That is, monitoring of the oscillations with light perturbs them and causes a gradually increasing deviation from the semiclassical picture.

At present we have no reliable quantitative argument to explain the particular Γt scaling of the measurement perturbations; say, why not Γt times some nonzero power of

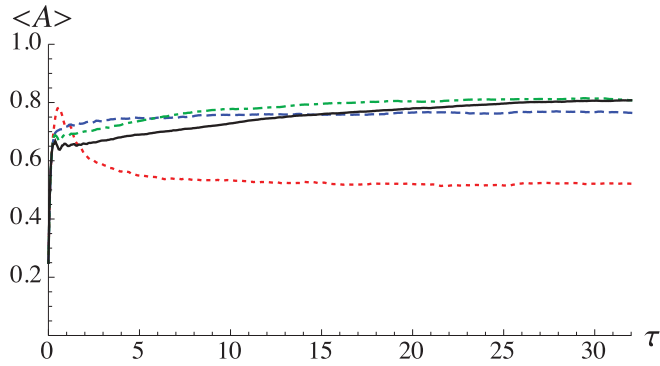


FIG. 7. (Color online) Average amplitude $\langle A \rangle$ as a function of the number of oscillation periods τ for the relatively small atom numbers $N = 2$ (dotted red line), $N = 4$ (dashed blue line), $N = 8$ (dash-dotted green line), and $N = 16$ (solid black line). The observation strength is $\gamma = 4$.

atom number N ? In fact, naively one would say that the number of photon counts in a time t , and therefore the measurement back-action, would be proportional to $N^2\Gamma t$. Obviously the back-action per atom is what counts and one would expect the scaling $N\Gamma t$, but that is not what we seem to observe. Mostly in the way of speculation, we note that even if the measurement is nominally about the squares of the atom numbers, it really probes atom numbers: The signal is proportional to $\Gamma t(N_b^2 - N_a^2) = \Gamma t(N_a + N_b)(N_b - N_a)$ where $N_a + N_b$ is a constant of the motion. It is conceivable that the back-action from the measurement of the difference of atom numbers is something akin to a phase $\simeq 1$, so that the back action in time t would be $\propto \Gamma t N$ and the back-action per atom would indeed be $\propto \Gamma t$.

Given that Josephson oscillations are associated with a BEC with nominally a large number of atoms in one quantum state, one naturally wonders how large does large have to be. We have studied this question in Fig. 7 for the atom numbers $N = 2$, $N = 4$, $N = 8$, and $N = 16$ by plotting $\langle A \rangle(\tau)$, the observation strength being $\gamma = 4$. $N = 2$ (dotted red line) behaves quite differently from the rest of the curves and $N = 4$ (dashed blue line) settles at a lower value than the remaining curves for $N = 8$ (dash-dotted green line) and $N = 16$ (solid black line). The surprising answer here is that $N = 8$, on the average four atoms in each potential well, is large enough that plots like this have the same qualitative character we find also for much larger atom numbers.

This point is further reinforced in Fig. 8, where we show the population imbalance $z(\tau)$, the inferred amplitude $A(\tau)$ (solid red line), and the inferred phase $\phi(\tau)/2\pi$ (dashed green line) for $N = 8$ and $\gamma = 4$ for one quantum trajectory. The data are genuinely random so any conclusions are really not warranted, but even for this small atom number the qualitative behavior of both plots is similar to the ones that are found at much larger atom numbers; see Fig. 3 for $N = 128$. Bayesian inference evidently is a Procrustean bed that tends to find oscillations. In fact, we argue even more broadly that a quantum-mechanical procedure intended to measure oscillations will produce oscillations. However, Bayesian inference will not report large-amplitude oscillations with a reasonably steady phase unless the counting rates

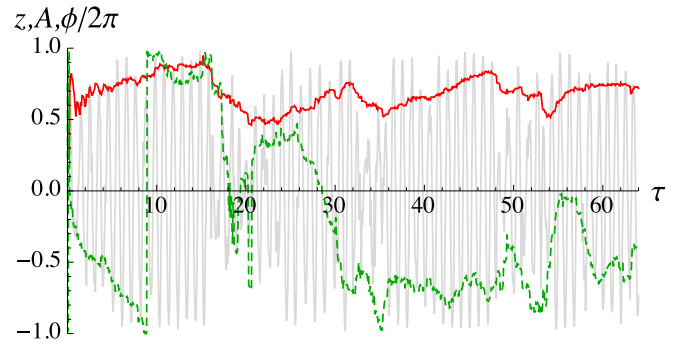


FIG. 8. (Color online) Oscillations of the population imbalance z , and the corresponding inferred amplitude A (solid red line) and phase $\phi/2\pi$ (dashed green line) as a function of time τ in one quantum trajectory for a small atom number $N = 8$. Here $\gamma = 4$. The sudden jump in the phase at about $\tau = 9$ is an artifact in that the phases $-\pi$ and π are actually the same.

indicate pronounced oscillations of the atoms between the traps. There is merit to the oscillations even for an atom number as small as $N = 8$.

V. CONCLUDING REMARKS

The basic technical assignment has been how to extract Josephson oscillations of the atoms between the sides of a double-well potential that purportedly follow from spontaneous breaking of the $U(1)$ gauge symmetry, given that the only observation data are photon counts due to light scattered from the two potential wells. We demonstrate how the parameters of the oscillations, amplitude and phase, may be obtained by Bayesian inference from the photon counts. The naive Bayesian inference turns out to be stiff on the face of the time-dependent oscillation amplitudes and phases, which we remedy by means of an algorithm that continuously broadens the inferred probability distribution of the oscillation parameters as the observations of photon counts go on.

In physics, Bayesian methods are typically used to infer parameters of a specific model from experimental data [29,30]. Here we are faced with the problem that there is no *a priori* model for the variations of the amplitude and phase of the oscillations. In response, we have devised what is in a sense a model-independent version of Bayesian inference. One could argue that our results depend on both the photon counts *and* the precise way in which Bayesian inference is carried out, including the broadening algorithm and its parameters. However, one could say the same of any standard application of Bayesian inference: The results depend on the choice of the model. Bayesian inference in principle comes with a way to compare quantitatively the likelihood of different models [29,30]. If, and how, this would work with our version remains to be seen.

Spontaneously broken symmetry is ordinarily thought to apply in the thermodynamic limit—in our terms, in the limit of an infinite number of atoms. The prediction would be steady oscillations with constant amplitude and phase. One way of formulating our physics question, very much analogously to

Ref. [5], is to ask what happens when the number of atoms is not infinite. We find a scaling law in the results that speaks of the number of photon counts needed to detect the oscillations, and another scaling law that presumably depends on quantum-mechanical back-action of the measurements affecting the oscillations. These constitute a quantitative characterization of the Josephson oscillations for a finite number of atoms.

As was demonstrated already early on [5–8,15], spontaneous breaking of gauge symmetry is not needed for observations of interference phenomena in condensates. Our viewpoint is that there is no spontaneously broken symmetry at all (either with condensates, or in other standard statistical-mechanics examples such models of a ferromagnet). Instead, the Josephson oscillations are created by the observation of the ...oscillations..., which makes correlations between the expected photon counts manifest. The mechanism, technically, is the quantum-mechanical back-action that modifies the state as a result of the already existing observations and ultimately leads to an illusion of spontaneous symmetry breaking.

In this regard the situation is different from the Bayesian inference procedures discussed in similar systems in the literature [36,37], where the goal is to find an objectively existing value of a parameter of the system, such as the tunneling amplitude J . In our view, the back-and-forth oscillations of the atoms do not reflect an existent property of the system at all, but are literally generated by the process of monitoring the oscillations.

It may be possible to infer the full evolving quantum state of the double-well system from the measurement record [38]. In the model of these authors the record consists of a continuous photocurrent not discrete photon counts as in our discussion, but as a matter of principle this difference is immaterial. By simply taking the times of photon counts from one simulation (call it experiment), we can force a parallel simulation (call it analysis) to reproduce the complete evolution of the quantum state in the original simulation. However, this observation does not render our classical Bayesian analysis superfluous. For one thing, in practice there would inevitably be lost photon counts

due to detector inefficiency. In simple numerical experiments we have found that our Bayesian method is not much affected by the loss of, say, half of the photons if the reduced detection efficiency is taken into account in the analysis. In contrast, what happens to a quantum analysis that slaves a simulation to an experiment (real or simulated) when not all scattered photons are detected is a question for future study.

The experiments we are simulating using quantum trajectories are obviously idealized to the extreme. For the time being we aim at points of principle, not designs of experiments. Nonetheless, we believe that our Bayesian inference scheme with the broadening procedure could find a place in the description of all sorts of observational data that come in individual photon counts or other discrete events, especially if every event has to be made to count. Such would be the situation, for instance, if the signal is inherently weak, or if the side effects of the events such as photon recoil are highly harmful.

As to the analysis of the Josephson oscillations, the main benefit of our Bayesian scheme is that it produces a time-dependent amplitude that can be averaged over a number of realizations. Since the oscillations are random, statistical averaging is the only way to describe them quantitatively. We have averaged, and have related the findings to physics principles that are after the fact quite obvious. The main surprise is that, even if the Josephson oscillations are traditionally associated with the notion of a BEC and consequently to a “large” number of atoms, the oscillations as seen through the lens of our Bayesian inference are similar starting from atom numbers as small as 8. In other words, four atoms in a potential well can already make a BEC. Experiments to probe classical-like behavior in this small and seemingly quantum-mechanical systems would evidently be very difficult, but might teach interesting lessons about the interface of quantum and classical physics.

ACKNOWLEDGMENTS

This work is supported in part by the National Science Foundation, Grants No. PHY-0967644 and No. PHY-1401151.

-
- [1] F. Dalfovo, S. Giorgini, L. P. Pitaevskii, and S. Stringari, *Rev. Mod. Phys.* **71**, 463 (1999).
 - [2] C. Kittel, *Introduction to Solid State Physics*, 6th ed. (Wiley, New York, 1986).
 - [3] B. Josephson, *Phys. Lett.* **1**, 251 (1962).
 - [4] J. Javanainen, *Phys. Rev. Lett.* **57**, 3164 (1986).
 - [5] J. Javanainen and S. M. Yoo, *Phys. Rev. Lett.* **76**, 161 (1996).
 - [6] Y. Castin and J. Dalibard, *Phys. Rev. A* **55**, 4330 (1997).
 - [7] J. I. Cirac, C. W. Gardiner, M. Naraschewski, and P. Zoller, *Phys. Rev. A* **54**, R3714 (1996).
 - [8] M. Naraschewski, H. Wallis, A. Schenzle, J. I. Cirac, and P. Zoller, *Phys. Rev. A* **54**, 2185 (1996).
 - [9] W. J. Mullin, R. Krotkov, and F. Laloë, *Am. J. Phys.* **74**, 880 (2006).
 - [10] W. J. Mullin and F. Laloë, *Phys. Rev. A* **82**, 013618 (2010).
 - [11] M. R. Andrews, C. G. Townsend, H.-J. Miesner, D. S. Durfee, D. M. Kurn, and W. Ketterle, *Science* **275**, 637 (1997).
 - [12] Z. Hadzibabic, S. Stock, B. Battelier, V. Bretin, and J. Dalibard, *Phys. Rev. Lett.* **93**, 180403 (2004).
 - [13] G. Cennini, C. Geckeler, G. Ritt, and M. Weitz, *Phys. Rev. A* **72**, 051601 (2005).
 - [14] G. Cennini, C. Geckeler, G. Ritt, and M. Weitz, *Phys. Rev. A* **77**, 013613 (2008).
 - [15] J. Ruostekoski and D. F. Walls, *Phys. Rev. A* **58**, R50 (1998).
 - [16] J. Dalibard, Y. Castin, and K. Mølmer, *Phys. Rev. Lett.* **68**, 580 (1992).
 - [17] R. Dum, P. Zoller, and H. Ritsch, *Phys. Rev. A* **45**, 4879 (1992).
 - [18] L. Tian and H. J. Carmichael, *Phys. Rev. A* **46**, R6801 (1992).
 - [19] S. Raghavan, A. Smerzi, S. Fantoni, and S. R. Shenoy, *Phys. Rev. A* **59**, 620 (1999).
 - [20] T. Spiller and J. Ralph, *Phys. Lett. A* **194**, 235 (1994).
 - [21] T. Brun, N. Gisin, P. O’Mahony, and M. Rigo, *Phys. Lett. A* **229**, 267 (1997).

- [22] T. Bhattacharya, S. Habib, and K. Jacobs, *Phys. Rev. Lett.* **85**, 4852 (2000).
- [23] A. J. Scott and G. J. Milburn, *Phys. Rev. A* **63**, 042101 (2001).
- [24] J. Javanainen, *Phys. Rev. A* **81**, 051602 (2010).
- [25] J. Javanainen and J. Ruostekoski, *New J. Phys.* **15**, 013005 (2013).
- [26] M. Albiez, R. Gati, J. Fölling, S. Hunsmann, M. Cristiani, and M. K. Oberthaler, *Phys. Rev. Lett.* **95**, 010402 (2005).
- [27] S. Levy, E. Lahoud, I. Shomroni, and J. Steinhauer, *Nature (London)* **449**, 579 (2007).
- [28] T. Zibold, E. Nicklas, C. Gross, and M. K. Oberthaler, *Phys. Rev. Lett.* **105**, 204101 (2010).
- [29] V. Dose, *Rep. Prog. Phys.* **66**, 1421 (2003).
- [30] U. von Toussaint, *Rev. Mod. Phys.* **83**, 943 (2011).
- [31] H. M. Wiseman and G. J. Milburn, *Quantum Measurement and Control* (Cambridge University Press, Cambridge, UK, 2010).
- [32] S. M. Yoo, J. Ruostekoski, and J. Javanainen, *J. Mod. Opt.* **44**, 1763 (1997).
- [33] G. Lindblad, *Commun. Math. Phys.* **48**, 119 (1976).
- [34] C. Gardiner and P. Zoller, *Quantum Noise*, 3rd ed. (Springer, Berlin, 2004).
- [35] W. H. Press, S. A. Teukolski, V. A. Vetterling, and B. P. Flannery, *Numerical Recipes: The Art of Scientific Computing*, 3rd ed. (Cambridge University Press, New York, 2007).
- [36] S. Gammelmark and K. Mølmer, *Phys. Rev. A* **87**, 032115 (2013).
- [37] A. Negretti and K. Mølmer, *New J. Phys.* **15**, 125002 (2013).
- [38] M. Hiller, M. Rehn, F. Petruccione, A. Buchleitner, and T. Konrad, *Phys. Rev. A* **86**, 033624 (2012).